

PHYSICS IN COLLISION - Stanford, California, June 20-22, 2002

PRECISION TESTS OF QCD AT HERA

David Milstead

Department of Physics, University of Liverpool, Liverpool, UK.

ABSTRACT

The electron-proton collider HERA has allowed the study of the partonic content of the proton in regions of Q^2 up to 50,000 GeV² and values of Bjorken- x down to 10^{-5} . This paper presents recent precision measurements of structure functions and hadronic final state observables which test QCD over this wide region of phase space.

arXiv:hep-ex/0210018v2 11 Oct 2002

1 Introduction

Deep-inelastic lepton-nucleon scattering experiments have traditionally shed light on the nature of the partons within the proton and the strong QCD interactions between them[1].

The ep scattering experiments H1 and ZEUS at the HERA facility at DESY have continued this tradition and have made precision measurements of both the inclusive ep scattering cross-section and features of the ep -induced hadronic final state. The theory of perturbative QCD, as implemented in the DGLAP[2] parton evolution equations, has been successful in describing these measurement at higher values of Q^2 (above $\approx 100 \text{ GeV}^2$). However, the DGLAP equations resum terms in $\ln(Q^2)$ and ignore terms in $\ln(1/x)$ which are expected to become important in the lower Q^2 , low x domain ($x \leq 10^{-3}$)[3]. Furthermore, gluon recombination effects may also be visible in the low x domain[4].

In a complementary way, the hadronic final state from ep collisions also offers a rich testing ground of QCD. High transverse momentum jet and particle production particles directly probe pQCD processes and reveal the partonic structure of the proton and photon. Hadron properties at low momentum are sensitive to the hadronisation process and can thus be used to assess the environmental dependence of fragmentation and test non-perturbative QCD models of hadron production.

This paper presents precision measurements of the proton structure F_2 and of hadronic final state observables.

2 The Proton Structure Function F_2 and the Gluon Momentum Distribution $xg(x)$ of the Proton

The reduced ep scattering cross-section σ_r can be written as a function of F_2 and F_L .

$$\sigma_r = \frac{d\sigma}{dx dQ^2} \cdot \frac{Q^4 x}{2\pi\alpha^2 Y_+} = F_2(x, Q^2) - \frac{y^2 F_L(x, Q^2)}{Y_+}$$

This quantity is dominated by the contribution from F_2 and F_L only plays an important role at large values of the inelasticity $y = \frac{Q^2}{sx}$.

Precision measurements of $F_2(x, Q^2)$ have been made by the H1[5] and ZEUS[6] collaborations. The ZEUS results are shown in figure 1 and compared with earlier fixed target data. The classic scaling violations of F_2 are exhibited via the strong dependence on Q^2 for a range of fixed x values. The low x behaviour of F_2 is dominated by quark anti-quark pair production arising from the gluon content $g(x)$ of the proton which, within the DGLAP formalism, is given by $F_2 \propto \alpha_s \cdot g(x)$. QCD

fits based on DGLAP evolution using the HERA data and the fixed target data are also shown. The fit describes the data well over several orders of magnitude in x and Q^2 . In the region of kinematic overlap the independent measurements from fixed target experiments and the ZEUS data agree well.

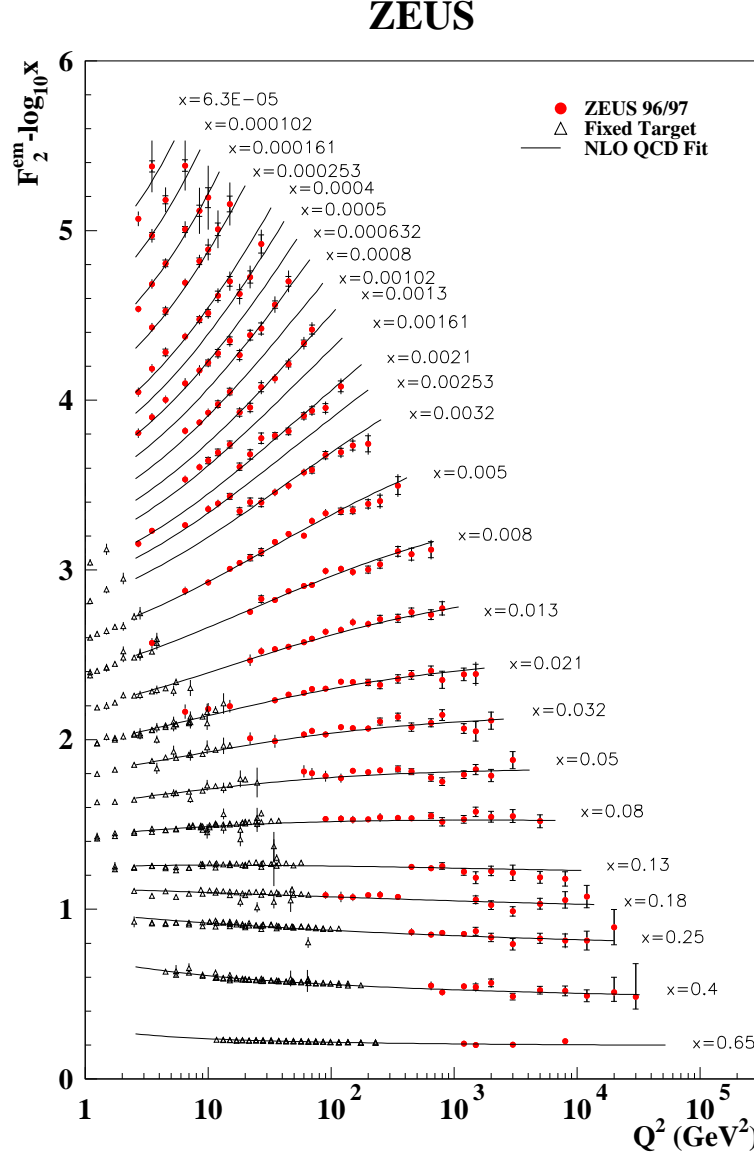


Figure 1: The proton structure function $F_2(x, Q^2)$ shown as a function of Q^2 for fixed values of x . QCD fits and results from fixed target experiments are also shown.

Using these precision measurements of the ep scattering cross-section and within the DGLAP formalism the gluon momentum distribution $xg(x)$ has been derived[7]. The dependence of $xg(x)$ on x for different values of Q^2 is shown in

figure 2. There is a strong rise towards low x for values of Q^2 down to about 5 GeV^2 . Below this, the gluon distribution tends to flatten off, approaching valence quark-like behaviour.

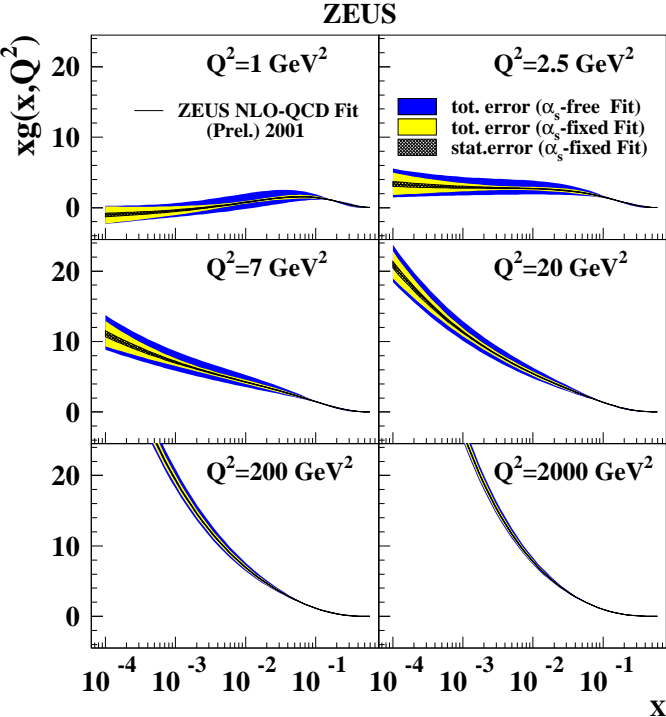


Figure 2: The gluon momentum distribution $xg(x)$ shown as a function of x at different values of Q^2 .

3 The Longitudinal Structure Function F_L

At high values of y the contribution from the longitudinal structure function F_L becomes significant. In figure 3, measurements of F_L from the H1 collaboration are presented as a function of x at different values of Q^2 .

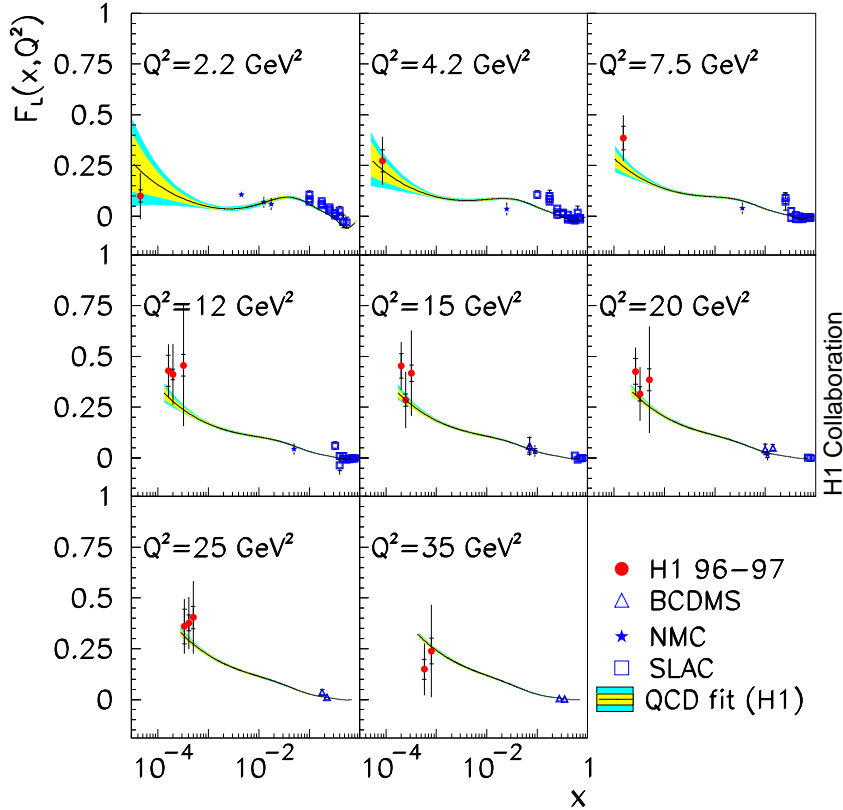


Figure 3: The longitudinal structure function F_L shown as a function of x at different values of Q^2 .

The values of $F_L(x, Q^2)$ increase towards low x , consistent with the QCD calculation which reflects the rise of the gluon momentum distribution.

The values of F_L were experimentally determined for $Q^2 < 10 \text{ GeV}^2$ following a procedure involving fitting straight lines in $\ln y$ to the derivative $\frac{\partial \sigma_r}{\partial \ln y}$ in order to estimate the contribution from the behaviour of F_2 to the reduced cross-section. For $Q^2 > 10 \text{ GeV}^2$, the NLO QCD fit in the low y domain ($y < 0.35$) is used to estimate F_2 in the high y region and thus extract F_L .

4 The Rise of F_2 Towards Low x

As mentioned in the introduction, the low x dependence of F_2 may be directly sensitive to any new physics which may be evident in this region of high partonic density[4].

Fits of the form $F_2(x, Q^2) = c(Q^2)x^{-\lambda(Q^2)}$ were made to the H1 structure function data[8].

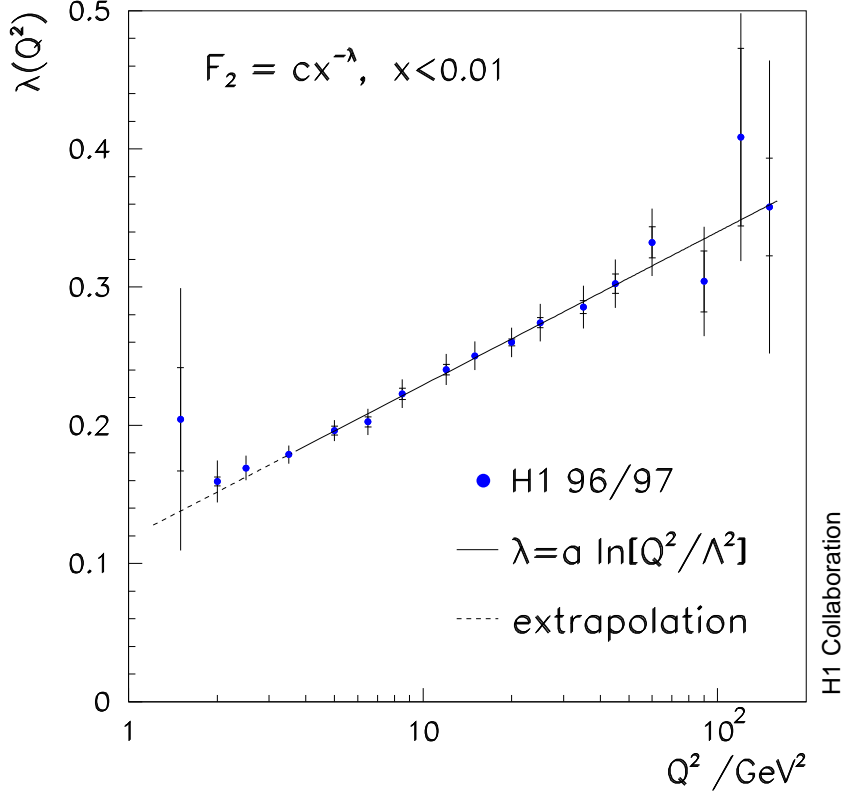


Figure 4: The dependence of λ on Q^2 .

The co-efficients $c(Q^2)$ were found to be approximately independent of Q^2 and, as shown in figure 4, $\lambda(Q^2)$ rises approximately linearly with $\ln Q^2$ and can be represented as $\lambda(Q^2) = a \cdot \ln[\frac{Q^2}{\Lambda^2}]$ with co-efficients $a = 0.0481 \pm 0.0013(stat) \pm 0.0037(syst)$ and $\Lambda = 292 \pm 20(stat) \pm 51(syst)$ MeV.

Below the deep-inelastic scattering region, for fixed $Q^2 < 1$ GeV², the simplest Regge phenomenology predicts that $F_2(x, Q^2) \propto x^{-\lambda}$ where $\lambda = \alpha_{pom(0)} - 1 \approx 0.08$ [9]. An extrapolation of the function $\lambda(Q^2)$ from the QCD fit gives a value of 0.08 at $Q^2 = 0.45$ GeV².

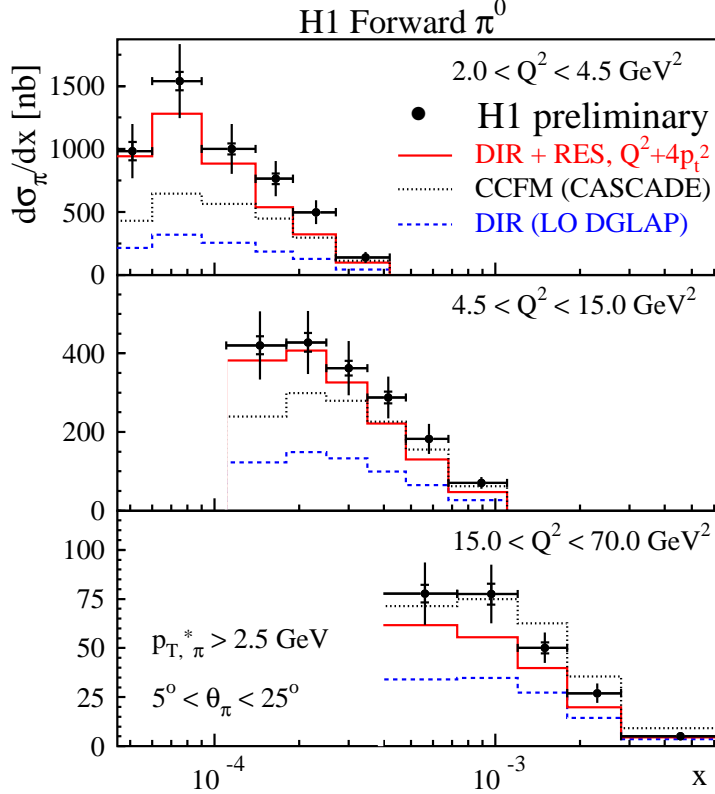


Figure 5: The forward π^0 cross-section as a function of Bjorken- x for different intervals of Q^2 .

5 Forward π^0 Production

The presence of particles with large values of transverse momentum (p_T) is indicative of a hard partonic sub-process and thus can be used to directly test pQCD calculations. It was therefore suggested that measurements of the forward π^0 cross-section could help to resolve one of the open questions at HERA: how do partons evolve from the proton? Parton evolution based on the DGLAP [2] equations successfully describes all inclusive measurements of the proton structure function F_2 . However, this scheme sums terms in $\ln(Q^2)$ and ignores terms in $\ln(1/x)$ which should play a significant role in the low Bjorken- x domain opened by HERA and therefore BFKL [3] evolution which, conversely, sums terms in $\ln(1/x)$ is expected to become applicable. Although measurements of F_2 offer no discrimination between the two schemes, the different dynamical features of the two approaches suggests that the hadronic final state may offer a means of observing BFKL effects. DGLAP evolu-

tion imposes a strong increasing ordering on k_T , the transverse momentum of the emitted parton and a weak decreasing ordering in the fractional momentum x of the propagating parton as the “ladder” develops away from the proton. However, BFKL evolution imposes a strong ordering in x and no ordering in k_T , allowing partons to take a ”random walk” in k_T and thus would give rise to more high momentum parton emissions than from DGLAP evolution.

It would then be expected that measurements of particle production in the region associated with this parton ladder would be sensitive to evolution effects. In fact, a series of hadronic final state measurements on transverse energy flow and jet and particle production in the forward (ie close to the proton) direction have already been made. A recent highlight of these works is the measurement of high p_T π^0 mesons [10]. These are made for π^0 mesons with values of transverse momentum in the photon-proton hadronic centre of mass system of $p_T > 2.5$ GeV. Values of the polar angle, θ , measured with respect to the incoming proton direction in the laboratory system were restricted to $5^\circ < \theta < 25^\circ$ and the laboratory system π^0 energy scaled by the incoming proton energy ($x_\pi = E_\pi/E_{proton}$) was required to be greater than 0.01. The deep inelastic scattering (DIS) kinematic range in Q^2 and the inelasticity variable, y , was restricted to $2 < Q^2 < 70$ GeV² and $0.1 < y < 0.6$.

Figure 4 shows the forward π^0 cross-section and as a function of Bjorken- x for three different intervals of Q^2 . The cross-section rises towards low Bjorken- x for each of the Q^2 ranges. Calculations based on DGLAP evolution from the proton alone fail to describe the data. Partonic structure can also be assigned to the resolved photon thus allowing DGLAP evolution from the photon and the proton. Calculations based on this picture are also shown [13] and they come close to the data although these fail at the highest measured of Q^2 . Calculations based on the CCFM equation which should interpolate between the DGLAP and BFKL regimes describes the data only in the highest Q^2 interval.

It is the author’s opinion that the next step for these analyses must be the exploitation of the full ep event information. One such proposed analysis is using multi-particle correlations which are directly sensitive to the presence or absence of strong k_T ordering in parton emissions [14]. The H1 and ZEUS experiments are strongly encouraged to pursue this.

6 Summary

Results on deep-inelastic ep scattering cross-sections in the low x regime at HERA have been presented. Perturbative QCD calculations based on DGLAP evolution

have been tested against precision results on proton structure functions and found to describe the data over many orders of magnitude in the kinematic variables x and Q^2 .

References

1. See, for example, M. Klein, *Structure Functions in Deep-Inelastic Lepton-Nucleon Scattering*, Proc. Lepton-Photon Symposium, Stanford, August 1999, World Scientific, ed. by J. Jaros and M. Peskin, p. 467, hep-ex/0001059 (2000).
2. Yu. L. Dokshitzer, Sov. Phys. JETP **46** (1977) 641;
V. N. Gribov and L. N. Lipatov, Sov. J. Nucl. Phys. **15** (1972) 438 and 675;
G. Altarelli and G. Parisi, Nucl. Phys. **B126** (1977) 298.
3. E. A. Kuraev, L. N. Lipatov and V. S. Fadin, Sov. Phys. JETP **44** (1976) 443;
E. A. Kuraev, L. N. Lipatov and V. S. Fadin, Sov. Phys. JETP **45** (1977) 199;
Y. Y. Balitsky and L. N. Lipatov, Sov. J. Nucl. Phys. **28** (1978) 822.
4. L. V. Gribov, E. M. Levin and M. G. Ryskin, Phys. Rep. **100** (1983) 1.
5. H1 Collaboration, C. Adloff *et al.*, Eur. Phys. J. **C21** (2001) 33.
6. ZEUS Collaboration, S. Chekanov *et al.*, Eur. Phys. J. **C21** (2001) 443.
7. ZEUS Collaboration, submitted paper 628, International Europhysics Conference on High Energy Physics, Budapest, Hungary, July 12-18, 2001.
8. H1 Collaboration, C. Adloff *et al.*, Phys. Lett. **B520** (2001) 183.
9. A. Donnachie and P. V. Landshoff, Z. Phys. **C61** (1994) 139.
10. C. Adloff *et al.*, Phys. Lett. **B462** 4401999.
11. J. Kwiecinski, A. Martin and J.J. Outhwaite *Eur. Phys. J. C* **9**, 1999 (611).
12. G. Ingelman, Proc. of the HERA workshop, eds W. Buchmüller and G. Ingelman, Hamburg (1992) Vol. 3, 1366.
13. H. Jung, Comp. Phys. Comm. **86**, 147 (1995) (for update see <http://www-h1.desy.de/~jung/rapgap/rapgap.html>).
14. E. de Wolf and P. Van Mechelen, Proc. of the Workshop on Monte Carlo Generators for HERA Physics, 1999, eds A.T. Doyle, G. Grindhammer, G. Ingelman and H. Jung.